



Queensland University of Technology
Brisbane Australia

This is the author's version of a work that was submitted/accepted for publication in the following source:

[Frost, Ray L.](#), Scholz, Ricardo, [López, Andrés](#), & [Theiss, Frederick L.](#)
(2014)

Vibrational spectroscopic characterization of the sulphate–halide mineral sulphohalite – implications for evaporites.

Spectrochimica Acta Part A: Molecular and Biomolecular Spectroscopy, 133, pp. 794-798.

This file was downloaded from: <https://eprints.qut.edu.au/73667/>

© Copyright 2014 Elsevier B.V.

NOTICE: this is the author's version of a work that was accepted for publication in *Spectrochimica Acta Part A*. Changes resulting from the publishing process, such as peer review, editing, corrections, structural formatting, and other quality control mechanisms may not be reflected in this document. Changes may have been made to this work since it was submitted for publication. A definitive version was subsequently published in *Spectrochimica Acta Part A*, [Volume 133, (10 December 2014)] DOI: 10.1016/j.saa.2014.06.008

Notice: *Changes introduced as a result of publishing processes such as copy-editing and formatting may not be reflected in this document. For a definitive version of this work, please refer to the published source:*

<https://doi.org/10.1016/j.saa.2014.06.008>

Vibrational spectroscopic characterization of the sulphate-halite mineral sulphohalite –implications for evaporites

Ray L. Frost^{a*}, Ricardo Scholz^b, Andrés López,^a Frederick L. Theiss^a

^a School of Chemistry, Physics and Mechanical Engineering, Science and Engineering Faculty, Queensland University of Technology, GPO Box 2434, Brisbane Queensland 4001, Australia.

^b Geology Department, School of Mines, Federal University of Ouro Preto, Campus Morro do Cruzeiro, Ouro Preto, MG, 35,400-000, Brazil

Abstract:

The mineral sulphohalite - $\text{Na}_6(\text{SO}_4)_2\text{FCl}$ is a rare sodium halogen sulphate and occurs associated with evaporitic deposits. Sulphohalite formation is important in saline evaporites and in pipe scales. Sulphohalite is an anhydrous sulphate-halide with an apparent variable anion ratio of formula $\text{Na}_6(\text{SO}_4)_2\text{FCl}$. Such a formula with oxyanions lends itself to vibrational spectroscopy. The Raman band at 1003 cm^{-1} is assigned to the $(\text{SO}_4)^{2-}$ ν_1 symmetric stretching mode. Shoulders to this band are found at 997 and 1010 cm^{-1} . The low intensity Raman bands at 1128 , 1120 and even 1132 cm^{-1} are attributed to the $(\text{SO}_4)^{2-}$ ν_3 antisymmetric stretching vibrations. Two symmetric sulphate stretching modes are observed indicating at least at the molecular level the non-equivalence of the sulphate ions in the sulphohalite structure. The Raman bands at 635 and 624 cm^{-1} are assigned to the ν_4 SO_4^{2-} bending modes. The ν_2 $(\text{SO}_4)^{2-}$ bending modes are observed at 460 and 494 cm^{-1} . The observation of multiple bands supports the concept of a reduction in symmetry of the sulphate anion from T_d to C_{3v} or even C_{2v} . No evidence of bands attributable to the halide ions was found.

Keywords: Raman spectroscopy, sulphohalite, sulphate, chloride, fluoride, infrared spectroscopy, evaporite

* Author to whom correspondence should be addressed (r.frost@qut.edu.au)
P +61 7 3138 2407 F: +61 7 3138 1804

Introduction

The mineral sulphohalite - $\text{Na}_6(\text{SO}_4)_2\text{FCl}$ is a rare sodium halogen sulphate and occurs associated with evaporitic deposits. The mineral was first described from Searles Lake, San Bernardino Co., California USA [1]. The crystal structure of sulphohalite has been determined [2]. The structure is cubic face-centered and there are four formula units in the unit cell, $a = 10.08(1) \text{ \AA}$ and latter redefined as space group $Fm\bar{3}m$, $a = 10.068(3) \text{ \AA}$ [3]. The crystal structure of sulphohalite was later compared with schairerite - $\text{Na}_3(\text{SO}_4)(\text{F},\text{Cl})$ by Fanfani et al [4]. There are four equivalent sulphate units in the crystal structure according to the X-ray diffraction results.

The Raman spectroscopy of the aqueous sulphate tetrahedral oxyanion yields the symmetric stretching (ν_1) vibration at 981 cm^{-1} , the in-plane bending (ν_2) mode at 451 cm^{-1} , the antisymmetric stretching (ν_3) mode at 1104 cm^{-1} and the out-of-plane bending (ν_4) mode at 613 cm^{-1} [5]. Ross reports the interpretation of the infrared spectra for potassium alum as ν_1 , 981 cm^{-1} ; ν_2 , 465 cm^{-1} ; ν_3 , $1200, 1105 \text{ cm}^{-1}$; ν_4 , 618 and 600 cm^{-1} [6]. Water stretching modes were reported at 3400 and 3000 cm^{-1} , bending modes at 1645 cm^{-1} , and librational modes at 930 and 700 cm^{-1} [7]. The authors have used vibrational spectroscopy to characterise a number of sulphate containing minerals [8-12].

The Raman spectrum of the mineral chalcantite shows a single symmetric stretching mode at 985 cm^{-1} . Two ν_2 modes are observed at 463 and 445 cm^{-1} and three ν_3 modes at 1173 , 1146 and 1100 cm^{-1} . The ν_4 mode is observed as a single band at 610 cm^{-1} . If two ν_1 peaks are observed, then this gives a strong indication that there are more than two sulphate units in the structure of the mineral. Multiple ν_2 and ν_4 bands support the concept that the symmetry of the sulphate anion is reduced in the mineral structure. Recently, the Raman spectra of four basic copper sulphate minerals, namely antlerite, brochantite, posnjakite and langite, are published [13]. The SO symmetric stretching modes for the four basic copper sulphate minerals are observed at $985, 990, 972$ and 974 cm^{-1} . The observation of differing band position wavenumbers suggests some sort of cation dependency of the position of the ν_1 band. Only the mineral brochantite showed a single band in this region. Multiple bands were observed for these minerals in the antisymmetric stretching region. The observation of

multiple bands in this spectral region supports the concept of a reduction in symmetry of the sulphate anion. Ross [6] lists the infrared spectra of the pseudo-alums formed from one divalent and one trivalent cations. Halotrichite has infrared bands at ν_1 , 1000 cm^{-1} ; ν_2 , 480 cm^{-1} ; ν_3 , 1121, 1085, 1068 cm^{-1} ; ν_4 , 645, 600 cm^{-1} . Pickeringite the Mg end member of the halotrichite-pickeringite series has infrared bands at ν_1 , 1000 cm^{-1} ; ν_2 , 435 cm^{-1} ; ν_3 , 1085, 1025 cm^{-1} ; ν_4 , 638, 600 cm^{-1} [6]. These minerals display infrared water bands in the OH stretching, 3400 and 3000 cm^{-1} region; OH deformation, 1650 cm^{-1} region; OH libration, 725 cm^{-1} region. Ross also reports a weak band at ~ 960 cm^{-1} which is assigned to a second OH librational vibration [6]. As with the infrared spectra, Raman spectra of alums are based on the combination of the spectra of the sulphate and water. Sulphate typically is a tetrahedral oxyanion with Raman bands at 981 (ν_1), 451 (ν_2), 1104 (ν_3) and 613 (ν_4) cm^{-1} [14]. Some sulphates have their symmetry reduced through acting as monodentate and bidentate ligands [14]. In the case of bidentate behaviour both bridging and chelating ligands are known. This reduction in symmetry is observed by the splitting of the ν_3 and ν_4 into two components under C_{3v} symmetry and three components under C_{2v} symmetry.

Raman spectroscopy has proven very useful for the study of minerals [15-28]. Indeed, Raman spectroscopy has proven most useful for the study of diagenetically related minerals where isomorphic substitution may occur as with rockbridgeite and beraunite, as often occurs with minerals containing sulphate groups. This paper is a part of systematic studies of vibrational spectra of minerals of secondary origin. The objective of this research is to report the Raman and infrared spectra of sulphohalite and to relate the spectra to the molecular structure of the mineral.

Experimental

Samples description and preparation

The sulphohalite sample studied in this work forms part of the collection of the Geology Department of the Federal University of Ouro Preto, Minas Gerais, Brazil, with sample code SAD-002. The mineral originated from Lake deposit, east of Trona, San Bernardino County, California (Type Locality for Sulphohalite).

The sample was gently crushed and the associated minerals were removed under a stereomicroscope Zeiss Stemi DV4 from the Museu de Ciência e Técnica - UFOP. The sulphohalite studied in this work occurs as single crystals with prismatic hexagonal form up to 5 mm. The mineral was identified with X-ray diffraction and the unit cell parameters were refined. Scanning electron microscopy (SEM) in the EDS mode was applied to support the mineral characterization.

Scanning electron microscopy (SEM)

Experiments and analyses involving electron microscopy were performed in the Center of Microscopy of the Universidade Federal de Minas Gerais, Belo Horizonte, Minas Gerais, Brazil (<http://www.microscopia.ufmg.br>). Sulphohalite crystals were coated with a 5nm layer of evaporated carbon. Secondary Electron and Backscattering Electron images were obtained using a JEOL JSM-6360LV equipment. Qualitative and semi-quantitative chemical analyses in the EDS mode were performed with a ThermoNORAN spectrometer model Quest and were applied to support the mineral characterization.

Raman microprobe spectroscopy

Crystals of sulphohalite were placed on a polished metal surface on the stage of an Olympus BHSM microscope, which is equipped with 10x, 20x, and 50x objectives. The microscope is part of a Renishaw 1000 Raman microscope system, which also includes a monochromator, a filter system and a CCD detector (1024 pixels). The Raman spectra were excited by a Spectra-Physics model 127 He-Ne laser producing highly polarized light at 633 nm and collected at a nominal resolution of 2 cm^{-1} and a precision of $\pm 1\text{ cm}^{-1}$ in the range between 200 and 4000 cm^{-1} . Repeated acquisitions on the crystals using the highest magnification (50x) were accumulated to improve the signal to noise ratio of the spectra. Raman Spectra were calibrated using the 520.5 cm^{-1} line of a silicon wafer. The Raman spectrum of at least 10 crystals was collected to ensure the consistency of the spectra.

It is noted that there is a Raman spectrum of sulphohalite given in the RRUFF data base. This spectrum has been downloaded and is provided in the supplementary information as Figure S1.

Infrared spectroscopy

Infrared spectra were obtained using a Nicolet Nexus 870 FTIR spectrometer with a smart endurance single bounce diamond ATR cell. Spectra over the 4000–525 cm⁻¹ range were obtained by the co-addition of 128 scans with a resolution of 4 cm⁻¹ and a mirror velocity of 0.6329 cm/s. Spectra were co-added to improve the signal to noise ratio.

Spectral manipulation such as baseline correction/adjustment and smoothing were performed using the Spectracalc software package GRAMS (Galactic Industries Corporation, NH, USA). Band component analysis was undertaken using the Jandel ‘Peakfit’ software package that enabled the type of fitting function to be selected and allows specific parameters to be fixed or varied accordingly. Band fitting was done using a Lorentzian-Gaussian cross-product function with the minimum number of component bands used for the fitting process. The Gaussian-Lorentzian ratio was maintained at values greater than 0.7 and fitting was undertaken until reproducible results were obtained with squared correlations of r^2 greater than 0.995.

Results and discussion

Chemical characterization

The SEM image of the mineral sample sulphohalite studied in this work is shown in Figure 1. The image shows a sulphohalite microcrystalline aggregate. Qualitative chemical analysis shows a homogeneous phase, composed of Na, Ca, S, Cl, F. Carbon was also observed and occurs due to C coating (Figure 2). A minor amount of Al was detected. .

Vibrational spectroscopy

The Raman spectrum of sulphohalite in the 100 to 4000 cm⁻¹ spectral range is displayed in Figure 3a. This figure shows the band position and the relative intensities of these Raman bands. There are large parts of the spectrum where no intensity is observed and therefore, the spectrum is subdivided into sections based upon the type of vibration being studied. The infrared spectrum of sulphohalite over the 500 to 4000 cm⁻¹ spectral range is reported in Figure 3b. This figure shows the position and relative intensity of the infrared bands. Again,

as for the Raman spectrum, the spectrum is subdivided into sections based upon the type of vibration being studied. The spectra shown in the figures have not been smoothed in any way and are the as obtained spectra. Some minor lack of signal may be observed.

The Raman spectrum of sulphohalite in the 900 to 1200 cm^{-1} spectral range is shown in Figure 4a. The infrared spectrum of sulphohalite in the 850 to 1200 cm^{-1} spectral range is shown in Figure 4b. The Raman band at 1003 cm^{-1} is assigned to the $(\text{SO}_4)^{2-}$ ν_1 symmetric stretching mode. Shoulders to this band are found at 997 and 1010 cm^{-1} . The first band may be assigned to a hot band. The second band is also attributed to the sulphate symmetric stretching mode, although it may be due to an overtone. In addition, a Raman band is noted at 1021 cm^{-1} . The observation of two bands supports the concept that there are two non-equivalent sulphate units in the structure of sulphohalite. An alternative explanation is that the observation of the two bands is due to Davydov splitting. The low intensity Raman bands at 1128, 1120 and even 1132 cm^{-1} are attributed to the $(\text{SO}_4)^{2-}$ ν_3 antisymmetric stretching vibrations. The Raman spectrum of sulphohalite downloaded from The RRUFF data base is shown in the supplementary information. This spectrum is in harmony with the spectrum reported in this work. The Raman peak at 1003 cm^{-1} in the RUFF spectrum, is assigned to the $(\text{SO}_4)^{2-}$ ν_1 symmetric stretching mode. The position of this band is in excellent agreement with the work reported here. In the RRUFF spectrum, a peak is observed at 1126 cm^{-1} and is assigned to the $(\text{SO}_4)^{2-}$ ν_3 antisymmetric stretching vibrations.

The infrared spectrum in the 900 to 1300 cm^{-1} spectral range of sulphohalite is shown in Figure 4b. The spectral profile is broad with a series of overlapping bands. A low intensity infrared band at 1003 cm^{-1} is assigned to the $(\text{SO}_4)^{2-}$ ν_1 symmetric stretching mode. The series of overlapping infrared bands at 1078, 1115, 1129 and 1157 cm^{-1} are ascribed to the $(\text{SO}_4)^{2-}$ ν_3 antisymmetric stretching vibrations.

The Raman spectra in the 400 to 700 cm^{-1} spectral range and in the 100 to 200 cm^{-1} spectral range are shown in Figure 5. The Raman bands at 635 and 624 cm^{-1} are assigned to the ν_4 SO_4^{2-} bending modes. Ross [7] investigated the infrared spectra of selected sulphate minerals and reported ν_4 SO_4^{2-} bending modes at 595, 618 and 680 cm^{-1} and ν_2 $(\text{SO}_4)^{2-}$ bending modes at 460 and 494 cm^{-1} . In the RRUFF spectrum, the Raman band at 635 cm^{-1} is attributed to the $(\text{SO}_4)^{2-}$ ν_4 bending mode.

182

183 The two Raman bands for sulphohalite at 467, 472 and 481 cm^{-1} are assigned to the ν_2
184 $(\text{SO}_4)^{2-}$ bending modes. In the RRUFF spectrum, the band at 470 cm^{-1} is ascribed to this
185 vibrational mode. The observation of multiple bands supports the concept of a reduction in
186 symmetry of the sulphate anion from T_d to C_{3v} or even C_{2v} . In the far low wavenumber
187 region, Raman bands are found at 109, 117, 146 and 159 cm^{-1} . These bands are best described
188 as external vibrations.

189 **Conclusions**

190 Raman spectroscopy combined with infrared spectroscopy has been used to study the mineral
191 sulphohalite, a mineral which is found in saline evaporites and in boiler scales. The mineral
192 may be readily determined using vibrational spectroscopy. However, Raman spectroscopy
193 proved more useful for the analysis of sulphohalite, no doubt because of the smaller spot size,
194 being the order of 1 micron as compare with infrared spectroscopy where the spot size is at
195 best around 25 microns.

196

197 The implication is that we can use Raman spectroscopy to readily analyses evaporite deposits
198 and scaling on pipes and in boilers. Raman spectroscopy can readily analysis sulphohalite
199 and related minerals and can distinguish sulphohalite from other minerals.

200

201 **Acknowledgements**

202 The financial and infra-structure support of the Discipline of Nanotechnology and Molecular
203 Science, Science and Engineering Faculty of the Queensland University of Technology, is
204 gratefully acknowledged. The Australian Research Council (ARC) is thanked for funding the
205 instrumentation. The authors would like to acknowledge the Center of Microscopy at the
206 Universidade Federal de Minas Gerais (<http://www.microscopia.ufmg.br>) for providing the
207 equipment and technical support for experiments involving electron microscopy. R. Scholz
208 thanks to Museu de Ciência e Técnica - UFOP

209

References

- [1] W.E. Hidden, J.B. Mackintosh, *Amer. J. Sc.* 36 (1888) 463-464.
- [2] A. Pabst, *Zeit. Krist.* 89 (1934) 514-517.
- [3] Y. Sakamoto, *J. Sc. Hiroshima Uni. Series A-2: Phys. Chem.* 32 (1968) 101-108.
- [4] L. Fanfani, A. Nunzi, P.F. Zanazzi, A.R. Zanzari, C. Sabelli, *Min. Mag.* 40 (1975) 131-139.
- [5] R.L. Frost, P.A. Williams, W. Martens, J.T. Klopogge, P. Leverett, *J. Raman Spectrosc.* 33 (2002) 260-263.
- [6] S.D. Ross, 6. S.D. Ross Chapter 18 pp 423 in *The infrared spectra of minerals*, V.C. Farmer editor. The Mineralogical Society London (1974). in *The infrared spectra of minerals*, Chapter 18 pp 423 (1974) The Mineralogical Society London.
- [7] S.D. Ross, *Inorganic Infrared and Raman Spectra* (European Chemistry Series), Wiley, London, 1972.
- [8] A. Lopez, R.L. Frost, Y. Xi, *Spectrochim. Acta, Part A*, (2014) Ahead of Print.
- [9] R.L. Frost, Y. Xi, R. Scholz, A. Lopez, A. Granja, *Spectrochim. Acta*, A109 (2013) 201-205.
- [10] R.L. Frost, R. Scholz, A. Lopez, Y. Xi, *Spectrochim. Acta*, A116 (2013) 165-169.
- [11] R.L. Frost, A. Lopez, Y. Xi, R. Scholz, L.M. Graca, L. Lagoeiro, *Spectrochim. Acta*, A112 (2013) 90-94.
- [12] R.L. Frost, A. Lopez, R. Scholz, Y. Xi, A.J. da Silveira, R.M.F. Lima, *Spectrochim. Acta*, A114 (2013) 85-91.
- [13] W. Martens, R.L. Frost, J.T. Klopogge, P.A. Williams, *J. Raman Spectrosc.* 34 (2003) 145-151.
- [14] R.L. Frost, J.T. Klopogge, P.A. Williams, P. Leverett, *J. Raman Spectrosc.* 31 (2000) 1083-1087.

- 235 [15] R.L. Frost, Y. Xi, K. Tan, G.J. Millar, S.J. Palmer, *Spectrochim. Acta*, A85 (2012) 173-
236 178.
- 237 [16] R.L. Frost, J. Cejka, J. Sejkora, J. Plasil, B.J. Reddy, E.C. Keeffe, *Spectrochim. Acta*,
238 A78 (2011) 494-496.
- 239 [17] R.L. Frost, E.C. Keeffe, *Spectrochim. Acta*, Part A, 81 (2011) 111-116.
- 240 [18] R.L. Frost, S.J. Palmer, *Spectrochim. Acta*, A78 (2011) 248-252.
- 241 [19] R.L. Frost, S.J. Palmer, *Spectrochim. Acta*, A78 (2011) 1255-1260.
- 242 [20] R.L. Frost, S.J. Palmer, *Spectrochim. Acta*, A78 (2011) 1250-1254.
- 243 [21] R.L. Frost, S.J. Palmer, *Spectrochim. Acta*, A79 (2011) 1794-1797.
- 244 [22] R.L. Frost, S.J. Palmer, *Spectrochim. Acta*, A79 (2011) 1215-1219.
- 245 [23] R.L. Frost, S.J. Palmer, *Spectrochim. Acta*, A79 (2011) 1210-1214.
- 246 [24] R.L. Frost, S.J. Palmer, S. Bahfenne, *Spectrochim. Acta*, A78 (2011) 1302-1304.
- 247 [25] R.L. Frost, S.J. Palmer, R.E. Pogson, *Spectrochim. Acta*, A79 (2011) 1149-1153.
- 248 [26] R.L. Frost, S.J. Palmer, Y. Xi, *Spectrochim. Acta*, A82 (2011) 132-136.
- 249 [27] R.L. Frost, S.J. Palmer, Y. Xi, *Spectrochim. Acta*, A83 (2011) 449-452.
- 250 [28] R.L. Frost, S.J. Palmer, Y. Xi, *Spectrochim. Acta*, A83 (2011) 444-448.

251

252

253

254

255

256

257

258 **List of Figures**

259 **Figure 1 - Backscattered electron image (BSI) of a sulphohalite crystal fragment up to**
260 **1.0 mm in length.**

261 **Figure 2 - EDS analysis of sulphohalite.**

262 **Figure 3 (a) Raman spectrum of sulphohalite over the 100 to 4000 cm⁻¹ spectral range**
263 **(b) Infrared spectrum of sulphohalite over the 500 to 4000 cm⁻¹ spectral range**

264 **Figure 4 (a) Raman spectrum of sulphohalite over the 900 to 1200 cm⁻¹ spectral range**
265 **(b) Infrared spectrum of sulphohalite over the 850 to 1200 cm⁻¹ spectral range**

266 **Figure 5 (a) Raman spectrum of sulphohalite over the 400 to 700 cm⁻¹ spectral range (b)**
267 **Raman spectrum of sulphohalite over the 100 to 200 cm⁻¹ spectral range**

268 **Figure 6 Infrared spectrum of sulphohalite over the 1200 to 1800 cm⁻¹ spectral range**

269

270

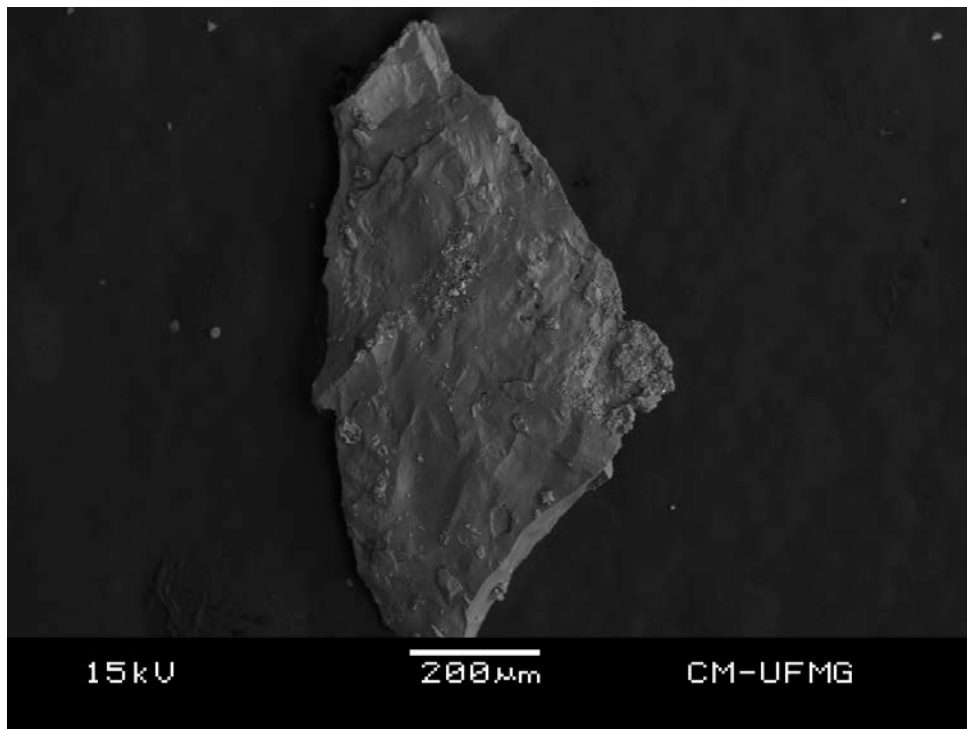


Figure 1 - Backscattered electron image (BSI) of a sulphohalite crystal fragment up to 1.0 mm in length.

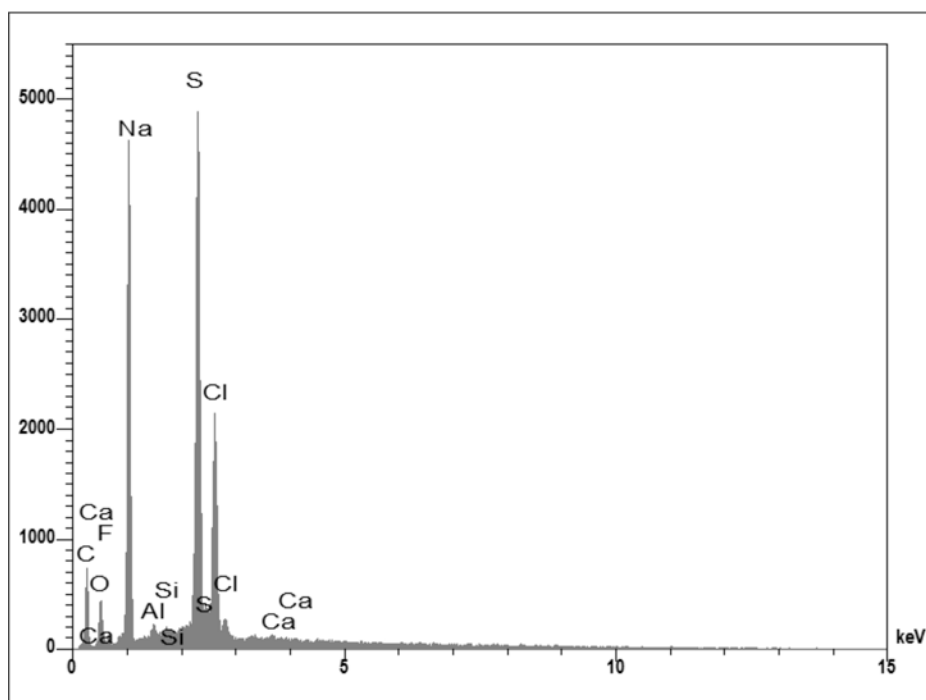
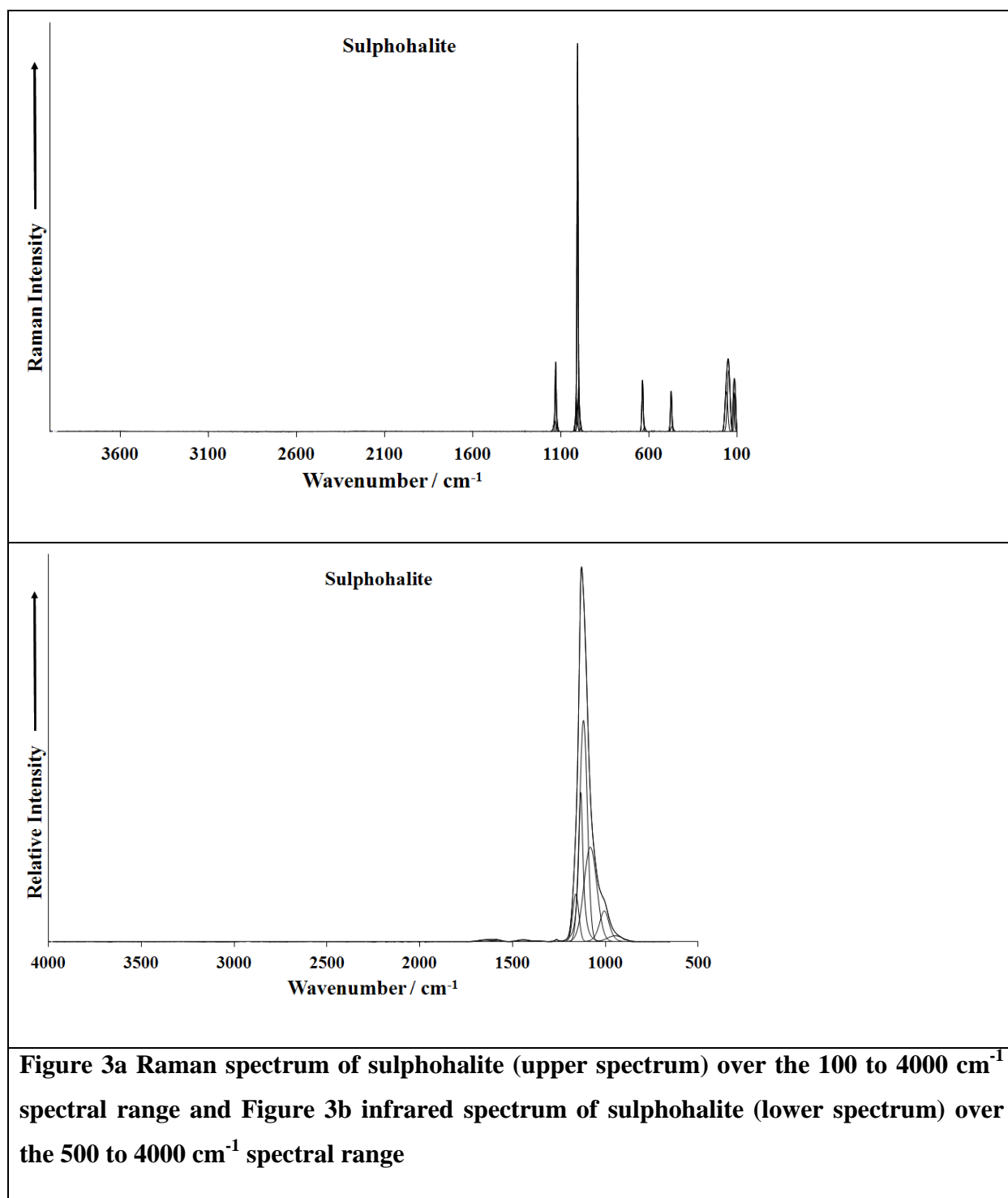


Figure 2 - EDS analysis of sulphohalite.

279

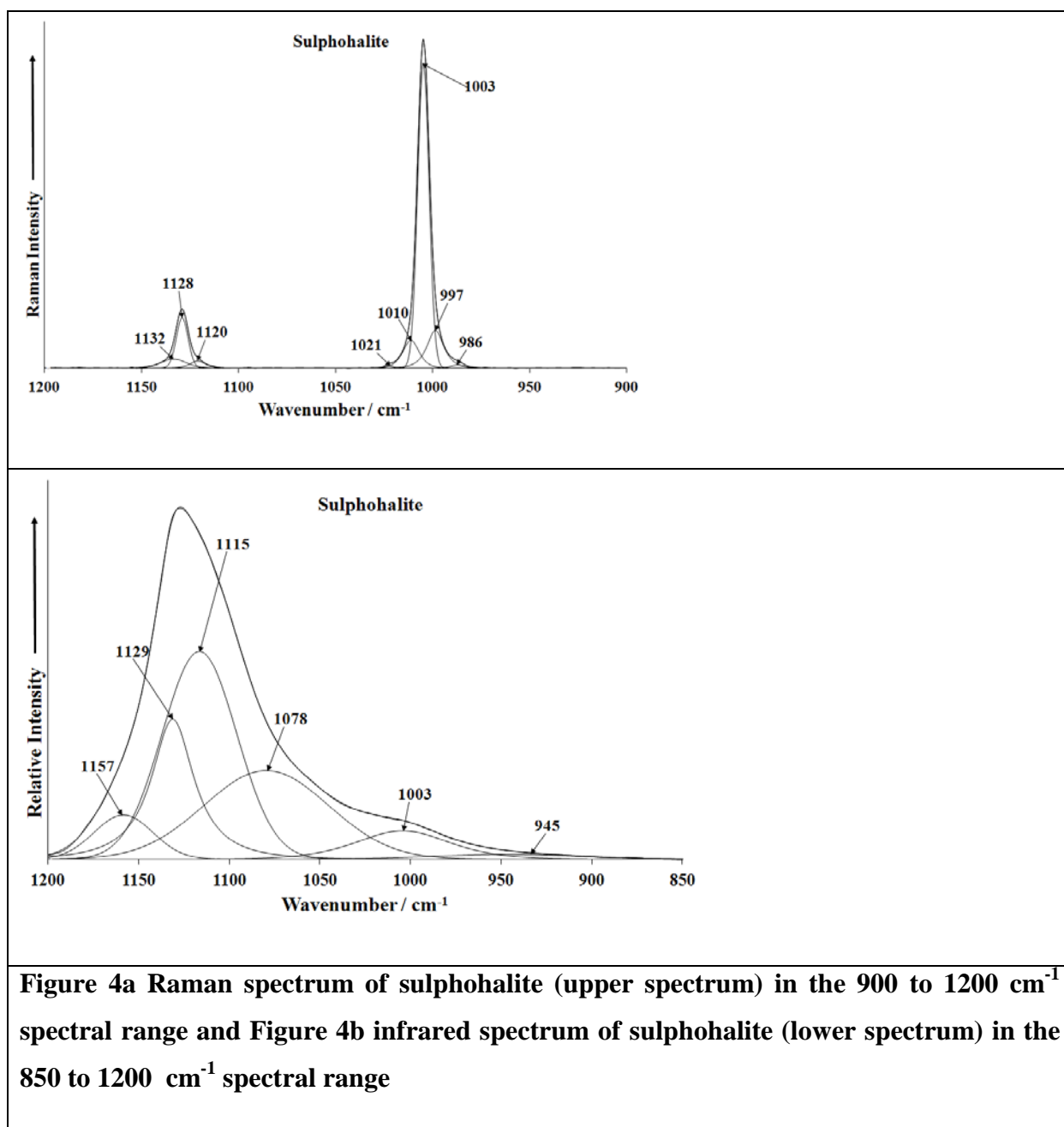
280



281

282

283



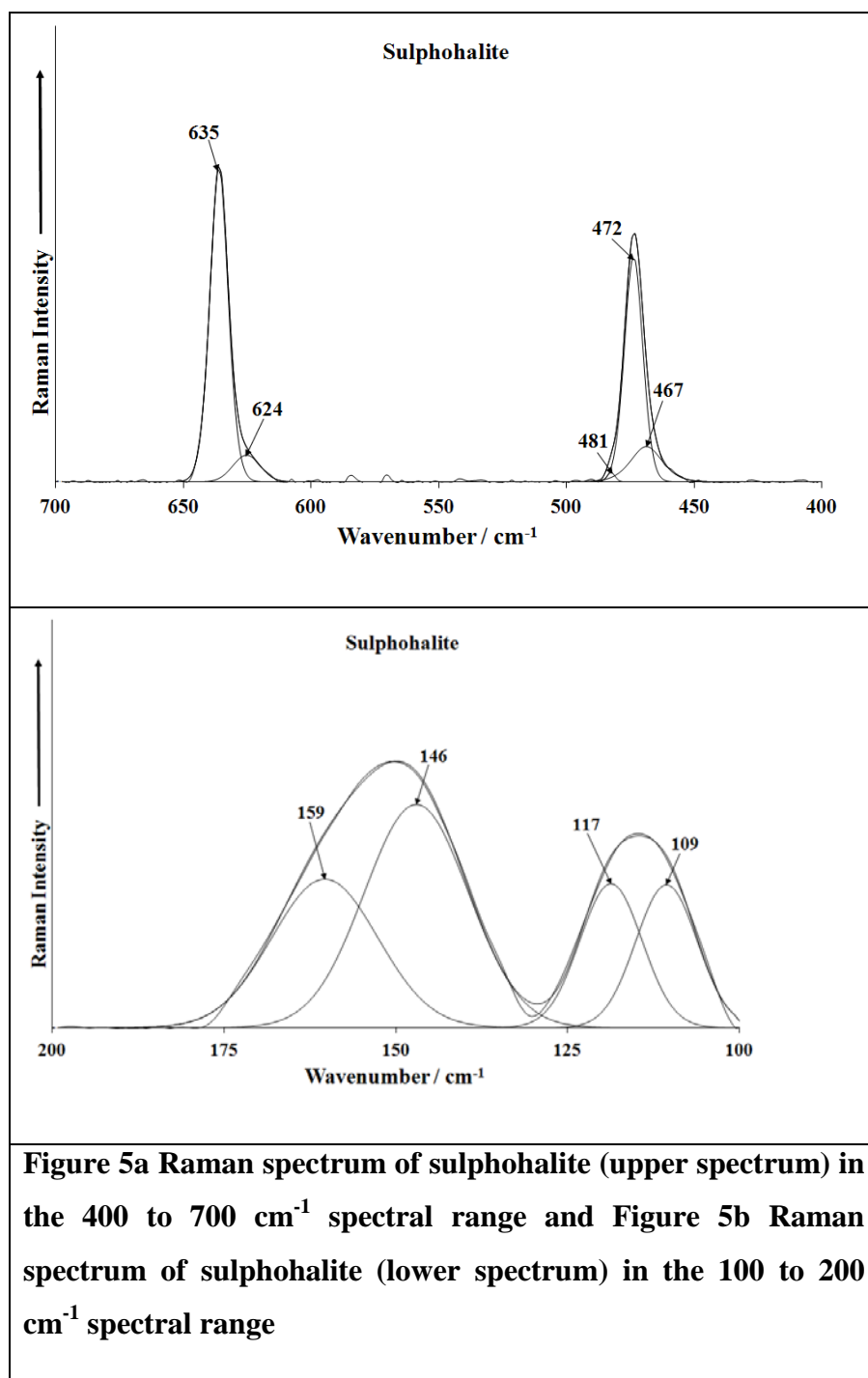
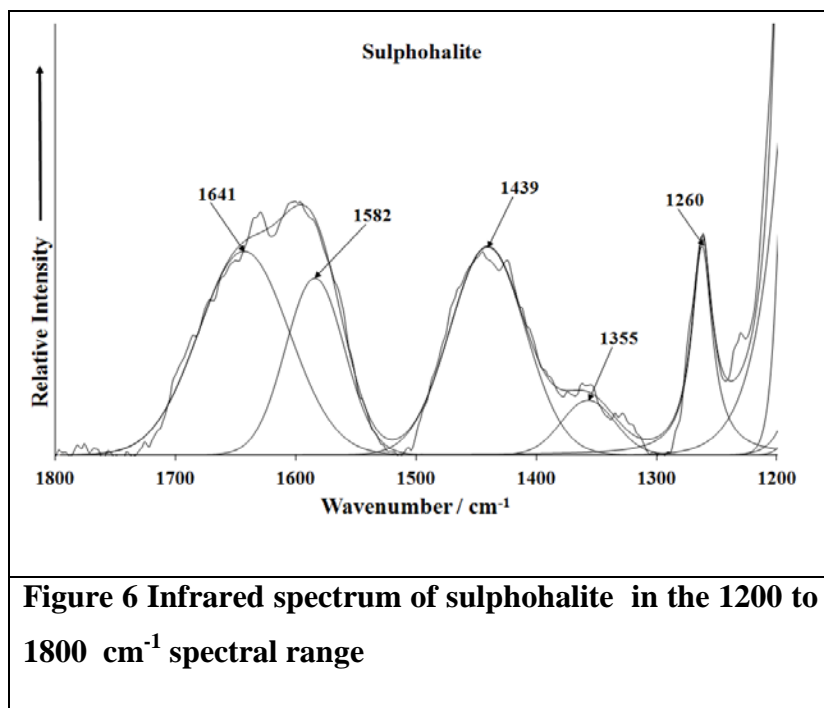


Figure 5a Raman spectrum of sulphohalite (upper spectrum) in the 400 to 700 cm⁻¹ spectral range and **Figure 5b** Raman spectrum of sulphohalite (lower spectrum) in the 100 to 200 cm⁻¹ spectral range

288



289

290

291

292

293

294

295

296